www.itcon.org - Journal of Information Technology in Construction - ISSN 1874-4753

A DEPLOYABLE SOLUTION FOR INDOOR TRACKING OF WORKERS IN CONSTRUCTION SITES THROUGH BLUETOOTH LOW ENERGY TECHNOLOGY

SUBMITTED: January 2023
REVISED: August 2025
PUBLISHED: September 2025
EDITOR: Robert Amor
DOI: 10.36680/j.itcon.2025.056

Mohammadali Khazen, Graduate Student
Dept. of Building, Civil & Environmental Engineering, Concordia University
mohammadali.khazen@mail.concordia.ca

Mazdak Nik-Bakht, Associate Professor
Dept. of Building, Civil & Environmental Engineering, Concordia University
mazdak.nikbakht@concordia.ca

Osama Moselhi, Professor
Dept. of Building, Civil & Environmental Engineering, Concordia University
osama.moselhi@concordia.ca

Jeffrey Dungen, Co-founder and Chief Executive Officer
ReelyActive Company
jeff@reelyactive.com

SUMMARY: *Real-Time Locating System (RTLS) using Bluetooth Low Energy (BLE) technology is becoming common to assist construction managers in making rational decisions pertinent to productivity monitoring and safety management on construction sites. However, there are still several challenges in deploying BLE-based RTLS on job sites. This paper proposes an RTLS explicitly designed for construction by satisfying requirements for widespread on-site adoption, including cost efficiency, scalability, and accuracy. The main contributions of this study are (i) substituting commonly used BLE receivers with BLE beacons; (ii) proposing a modular infrastructure placement strategy; (iii) developing localization algorithms using triangulation technique; (iv) post-processing the worker's estimated locations. The experimental results show a localization error of 0.56 (m) and 0.64 (m) in a middle-size indoor space when the target is dynamic and static, respectively. This level of accuracy is an improvement compared to that reported in the literature and can be considered appropriate for most worker tracking applications on construction job sites. Moreover, replacing traditional BLE receivers that are smartphones or devices that require electrical wiring with battery-powered BLE beacons, and using the modular infrastructure placement strategy improved the RTLS scalability and efficiency in implementation cost and power consumption. The impact of environmental conditions, such as the weather availability of metal and construction equipment, on the developed RTLS's performance, must be studied in future works.*

KEYWORDS: *Real-Time Locating System (RTLS), Bluetooth Low Energy (BLE), Triangulation, machine learning, indoor locating system.*

REFERENCE: *Mohammadali Khazen, Mazdak Nik-Bakht, Osama Moselhi & Jeffrey Dungen (2025). A Deployable Solution for Indoor Tracking of Workers in Construction Sites through Bluetooth Low Energy Technology. Journal of Information Technology in Construction (ITcon), Vol. 30, pg. 1377-1397, DOI: 10.36680/j.itcon.2025.056*

1. INTRODUCTION

Sensor-based tracking systems for construction sites can potentially change the business processes on the job sites by providing automated data acquisition and analysis for productivity and safety, among other applications (Umer and Siddiqui, 2020). Traditionally, on-site monitoring techniques primarily depend on manual processes that are time-consuming and error-prone (Park and Brilakis, 2016). However, many state-of-the-art technologies have been applied lately to effectively assist construction managers and safety inspectors in making rational decisions supporting the management of daily construction activities and site monitoring (Park *et al.*, 2017). Recent studies have highlighted that indoor localization applications can effectively manage the worksite (Becerik-Gerber *et al.*, 2014)(Umer and Siddiqui, 2020). The recent use of Real-Time Locating Systems (RTLS) focusing on the geographical mapping of worker locations results in trajectories to quantify the time spent in specific workspaces (Umer and Siddiqui, 2020). Hence, construction worker tracking on construction sites allows identification and tracking of the workforce to support effective progress monitoring, activity sequence analysis, and productivity measurements, as well as enhancing site safety management (Park *et al.*, 2012).

Several IoT (Internet of Things) technologies are commonly used by indoor tracking solutions, including Bluetooth Low Energy (BLE), Radio Frequency Identification (RFID), and Ultra-Wideband (UWB) technologies (Moselhi *et al.*, 2020)(Kim *et al.*, 2019)(Costin *et al.*, 2012). Also, there are less commonly used alternatives for indoor localization, including embedded sensors, Lidar and laser scanning, high-resolution video camera, digital photogrammetry, and WiFi (Umer and Siddiqui, 2020),(Alishahi *et al.*, 2021). The BLE technology-based system uses transmitters/receivers attached to the walls or ceilings of indoor environments to estimate the location of the target node. A BLE-based system comprises a receiver and transmitter that can wirelessly communicate. The BLE receiver is either fixed in a known location or worn by the workers, and it can capture the Received Signal Strength Indicator (RSSI) from the beacons to estimate the worker's location (Kunhoth *et al.*, 2019)(Zhuang, 2020).

BLE is considered the most cost-effective among other IoT-based technologies and appears reasonably accurate for many indoor localization applications in the construction domain (Zhao *et al.*, 2019) (Zhuang *et al.*, 2016). Hence, BLE technology is used in this study to develop RTLS. Nevertheless, while BLE solutions have been widely explored, they often rely on high-cost AC gateways or smartphone receivers (Park *et al.*, 2017; Li et al., 2019; Sou et al., 2019). These configurations introduce practical challenges, such as wiring requirements, data privacy concerns, and the need for frequent maintenance of personal devices.

This paper addresses these limitations by proposing one of the first fully beacon-based RTLS implementations for construction environments. By using BLE beacons for both reference nodes and worker-worn devices, the system eliminates the need for expensive gateways or smartphones, reducing costs and simplifying deployment. While prior work such as Park et al. (2017) demonstrated BLE deployments integrated with BIM for worker tracking, their system relied on fixed AC-powered gateways and a more static infrastructure layout. In contrast, our proposed system uses battery-powered beacons with a modular placement strategy, significantly reducing wiring needs and enhancing deployability on evolving construction sites. This makes the system easier to scale, relocate, and maintain under real-world construction conditions.

The main goal of the present paper is to propose the hardware/software infrastructure and analysis models for tracking workers on dynamic construction sites. A novel RTLS is proposed, specialized for tracking workers on construction sites to address some of the existing gaps with respect to deployability, layout dynamism, and accuracy of tracking systems. In this regard, after a review of the literature on the localization techniques and the type of devices used in BLE-based RTLS, the gaps are identified, and objectives are set up. Then, the components of the proposed RTLS, including infrastructure placement strategy, RSSI-distance model, localization estimation model, and estimated locations post-processing models, are introduced. Finally, the details of the experimental study and performance of the proposed RTLS are provided.

2. LITERATURE REVIEW

Indoor localization has been extensively studied in construction environments to improve safety, resource tracking, and operational efficiency. Several technologies, including UWB, RFID, and BLE, have been investigated for real-time localization. Each technology offers unique capabilities and trade-offs, as summarized in Table 1 which provides an overview of RTLS technologies in terms of accuracy, testbed environments, and hardware configurations.

Table 2: Summary of RTLS technologies in construction environments.

Authors	Technology	Testbed dimensions (m × m)	Testbed Environment	Installed Devices On-Site	Target Object State	Accuracy (m)
(Umer and Siddiqui, 2020)	UWB	40.0 × 55.0	Open outdoor without obstacles	4 UWB receivers	Stationary	MAE = 0.18
(Sadowski et al., 2020)	UWB	13.4 × 9.6	Laboratory with metallic surfaces	4 UWB receivers	Mobile	MAE = 0.30
(Kim and Han, 2018)	RFID	30.0 × 30.0	Basement of an ongoing apartment	4 RFID readers	Mobile	MAE = 1.27
(Montaser and Moselhi, 2013)	RFID	75.2 m2	Cast-in-place concrete building	24 tags RFID	Mobile	MAE = 1.00
(Mohsin et al., 2019)	BLE	10.0 × 5.0	Room with obstacles	12 beacon	Stationary	MAE = 1.28
(Park and Cho, 2017)	BLE	6.0 × 3.0	Office with obstacles	4 beacon	Stationary	MSE = 0.70

As seen from the table, UWB technology can provide a high positioning accuracy, with an error of as low as 18 (cm). The BLE and RFID technologies can also deliver a reasonable level of localization accuracy by assigning more devices per unit area on the job sites. Due to the high positioning accuracy of UWB, it is generally used in construction activities that require a higher level of positioning accuracy, including critical crane lifts and off-site fabrication (Umer and Siddiqui**,** 2020). Another application of using UWB is construction resource (worker and equipment) tracking leading to safety monitoring practices by introducing safety boundaries and danger zones (Sadowski et al., 2020). Regarding safety management, RFID technology can also be used to provide decision-makers with a warning if a worker is in proximity to hazardous areas (Kim and Han, 2018). However, the most used application of RFID is the localization of assets to derive knowledge about construction project status (Montaser and Moselhi**,** 2013). Despite its benefits, RFID's reliance on extensive hardware and its susceptibility to interference make it less ideal for frequently changing construction environments.

BLE technology has gained significant attention in recent years due to its low cost, energy efficiency, and adaptability in dynamic environments. While BLE systems generally have lower accuracy than UWB, their scalability and ease of deployment make them ideal for applications that require frequent infrastructure relocation. By increasing beacon density or employing advanced signal processing algorithms, BLE can achieve sufficient accuracy for many construction applications.

Building on this foundation, Table 3 delves deeper into BLE-based RTLS studies, highlighting testbed dimensions, reference devices, and localization techniques. This table provides a detailed comparison of BLE systems developed since 2017, emphasizing the importance of contextual differences in evaluating their performance. Since a direct comparison of those systems only based on their accuracy will not be precise due to the contextual differences among the experiments, specifications related to the studies' testbeds and their hardware requirements are also considered. The table consists of evaluation metrics including (i) testbed dimensions, representing the dimensions of the RTLS coverage area; (ii) type of reference devices, introducing the type of fixed BLE devices used as reference nodes in the testbed; (iii) number of the reference devices, showing the number of fixed BLE devices used as reference nodes in the testbed; (iv) type of device worn by the target, representing the BLE tracking device worn by the worker; (v) accuracy, identified through the localization error of the RTLS; and (vi) localization techniques in the RTLS: representing the used localization techniques.

BLE systems have been applied to various construction scenarios, with several studies demonstrating innovative techniques to improve localization performance. For example, Gómez-de-Gabriel et al. (2018) investigated BLE beacons for monitoring harness use on construction sites. Their approach utilized RSSI measurements combined with Extended Kalman Filters, providing a robust and relocatable solution in dynamic environments. The system did not require extensive calibration or external processing support, which is highly beneficial in construction settings where frequent infrastructure relocation is needed. However, its precision is still limited by the inherent variability of RSSI signals.

Dror et al. (2019) evaluated BLE-based worker tracking with two configurations: mobile beacons with fixed gateways and fixed beacons with mobile gateways. While the study demonstrated BLE's potential for construction sites, it also highlighted challenges in achieving consistent accuracy in dynamic and obstructed environments, emphasizing the need for strategic placement of beacons and gateways. Similarly, Bai et al. (2020) proposed a low-cost BLE-based indoor positioning system using Raspberry Pis for data collection and processing. The system combined trilateration and fingerprinting techniques and employed noise reduction algorithms like Kalman and Particle Filters to improve accuracy. Their findings highlighted the critical influence of beacon placement and filtering algorithms on localization performance in construction scenarios. Bencak et al. (2022) introduced a nature-inspired optimization algorithm for BLE beacon placement, demonstrating improved localization precision in warehouse environments. While primarily focused on intralogistics, the findings are adaptable to construction sites, where frequent infrastructure relocation and optimization are common.

Table 4: Summary of relevant related research work.

Authors	Testbed dimensions (m × m)	Type of reference devices	No. of reference devices	Type of devices worn by the target	Accuracy (m)
Fingerprinting Technique					
(D. Sun et al., 2021)	14.0 × 12.0	AC Gateway	13	BLE Beacon	MAE = 0.97
(Li et al., 2019)	8.0 × 8.0	AC Gateway	4	Smartphone	RMSE = 1.00
(Sou et al., 2019)	7.1 × 4.2	BLE Beacon	9	Smartphone	MAE = 1.12
(Dinh et al., 2020)	25.0 × 15.0	Raspberry Pi & BLE Beacon	13	Smartphone	MAE = 1.18
(X. Sun et al., 2021)	80 m²	BLE Beacon	26	Smartphone	MAE = 1.23
(Castillo-Cara et al., 2017)	4.0 × 3.0	BLE Beacon	5	Smartphone	MAE = 1.93
(Taşkan and Alemdar, 2021)	14.0 × 11.0	AC Gateway	3	BLE Beacon	MAE = 2.58
Trilateration Technique					
(Huang et al., 2019)	8.8 × 5.6	BLE Beacon	8	Smartphone	RMSE = 0.76
(Baek and Cha, 2019)	8.0 × 3.5	AC Gateway	6	BLE Beacon	MAE = 1.78
(Cantón Paterna et al., 2017)	8.7 × 6.2	SBC (Raspberry Pi)	4	BLE Beacon	90% below 1.82
(Sadowski et al., 2020)	6.0 × 5.5	SBC (Raspberry Pi)	3	BLE Beacon	MSE = 2.98

Despite the advancements in BLE-based RTLS, critical factors in developing such systems for construction sites have not been carefully considered. Firstly, the existing BLE-based RTLS relies on mobile phones and Direct Current (DC) electronics needing electrical wiring to operate. This reliance can cause interference with the construction workflow of job sites and adversely affect workers' hazard recognition (Umer and Siddiqui, 2020),(Sattineni and Schmidt, 2015). Secondly, previous research studies lack an infrastructure placement strategy that is adaptable to construction environments where infrastructure must be relocated frequently. Thirdly, BLE technology has not provided an impressive level of accuracy based on the numbers reported in the literature, so it may not be suitable for safety-related applications (Umer and Siddiqui, 2020)(Kunhoth *et al.*, 2020).

However, several gaps remain. BLE signals are highly susceptible to environmental interference, such as metal obstructions, multipath effects, and crowded conditions, which reduce reliability (Castillo-Cara et al., 2017); (Taşkan and Alemdar, 2021). Existing systems often struggle with frequent infrastructure relocation demands on dynamic sites and exhibit inconsistent accuracy due to variations in experimental setups (Baek and Cha, 2019; Cantón Paterna et al., 2017). Fingerprinting methods, while accurate, require extensive and costly calibration, making them unsuitable for environments with frequent changes (Castillo-Cara et al., 2017). Furthermore, BLE-based RTLS systems face challenges in dense Bluetooth environments, where high signal variability and processing inefficiencies can lead to errors (Huang et al., 2019; X. Sun et al., 2021). Addressing these gaps is essential to enhance the performance and deployability of BLE-based RTLS in real-world scenarios.

To address some of these gaps, in the present study, modular infrastructure and a novel beacon-based tracking system are implemented, and algorithms are developed to locate workers on the job site accurately. This advancement will be a step forward in adopting RTLS in the construction industry. Cost efficiency, scalability, and accuracy are the three primary criteria for developing the system; accordingly, the following objectives are

considered for the study. (i) Proposing an RTLS architecture with minimal dependency on wiring and electricity outlets; (ii) Developing an algorithm to overcome the limitation of the restricted payload size of a BLE packet that allows the receiving beacon to broadcast only three detected transmitters at a time. (iii) Proposing a modular BLE beacon placement strategy consisting of repetitive modules similar in size, shape, and device placement. (iv) Categorizing the measurements of positions and distances of the transmitter from the receiver and developing a localization algorithm for each category. (v) Applying a set of post-processing steps, including filtering techniques, on the estimated locations to mitigate the system's incoherent computed locations, and (vi) Investigating the RTLS performance for various beacon placements on a human body. It is essential to emphasize that the infrastructure proposed in this paper was later used in combination with data fusion techniques for location, body orientation, and productivity state detection, to study worker behavior and production monitoring in repetitive construction activities (Khazen et al., 2024). While that publication focuses on high-level behavioral and productivity monitoring, the present paper details the foundational hardware and software developments of the BLE-based RTLS infrastructure that enabled it, with a focus on system design, deployment strategy, and validation under dynamic construction conditions.

3. PROPOSED REAL-TIME LOCATING SYSTEM (RTLS)

In the proposed architecture here, the fixed and mobile nodes are the transmitter and receiver, respectively. This enables the system infrastructure to be fully wireless (except for the gateways; on average one per every 900m^2) and independent of smartphones which increases the deployability of the RTLS in the construction domain. The system has been designed so that a receiving beacon (transceiver) worn by a worker receives BLE signals from the closest three reference beacons on a construction site and transfers them to a cloud database through a gateway. This section describes the hardware, software, and algorithms deployed in the proposed RTLS.

3.1 General Architecture of the System

The system's communication architecture comprises four main components, i.e., Data Advertisement; Data Reception; Data Transfer; and Cloud Computing. The *Data Advertisement* component comprises transmission beacons fixed in the space, the primary function of which is to broadcast radio signals (BLE packets) that cover a particular area. The *Data Reception* component consists of a receiver (R) worn or carried by the workers, which captures the packets from the transmitter (T), with an RSSI proportional to their distance, and adds that information to the packet. The *Data Transfer* module is a gateway (G) that transmitted the information (packet) collected by the receiver back to a central cloud computing system via WiFi. Last but not least, *Cloud Computing* stores data packets in a database through which the RTLS models process the data (Mohsin *et al.*, 2019). In the proposed RTLS, the fixed reference transmitter periodically broadcasts signal data to the wearable receiving beacon through the data BLE packet. Simultaneously, upon receiving the beacon BLE advertising packet from the transmitter, the wearable receiving beacon read the RSSI value using its radio circuitry. Then, the wearable receiving beacon forwards the measured RSSI data encapsulated in a data BLE advertising packet (collected from the transmitter) to the gateway. The overview of the communication architecture of the proposed system is shown in Figure 1 (a).

The developed RTLS algorithms generate three models: (i) RSSI-distance estimation model; (ii) Localization estimation model; and (iii) Localization post-processing model. It is noted that the system is to be used for tracking workers (and not other objects on the site), with a height typically ranging from 155 to 205 cm. The system provides two dimensions (2D) location coordinates of workers. By identifying the floors on which the workers are located, using the reference transmitter Identities (ID)s, workers can be then tracked in the 3D space of the job site. Furthermore, the system is developed and tested for indoor environments where components of a target building (e.g., foundation, slabs) are already erected. Tracking workers in indoor environments is more challenging than in outdoor environments due to the absence of Global Positioning System (GPS) signals and line of sight (LoS) with orbiting satellites (Kunhoth *et al.*, 2020).

In line with existing studies, each step of our RTLS development was informed by relevant data and prior research. For instance, adopting minimal wiring and smartphone-free receivers stems from the need to reduce on-site disruptions (Dror et al., 2019) and interference concerns (Park et al., 2017). Our restricted-payload algorithm leverages findings on BLE packet size limitations (Sun et al., 2021), while the proposed modular placement strategy aligns with calls for frequently relocatable infrastructures (Bencak et al., 2022; Gómez-de-Gabriel et al., 2018). The record-correction approach to handle Semi- and Non-logical signals builds on studies addressing RSSI

fluctuation due to multipath (Cantón Paterna et al., 2017). Finally, incorporating multiple post-processing techniques (SMA, ES, Kalman) draws on widely referenced filtering practices in localization (Sou et al., 2019; Mackey et al., 2020), ensuring that each key methodology component reflects proven methods or recognized industry needs.

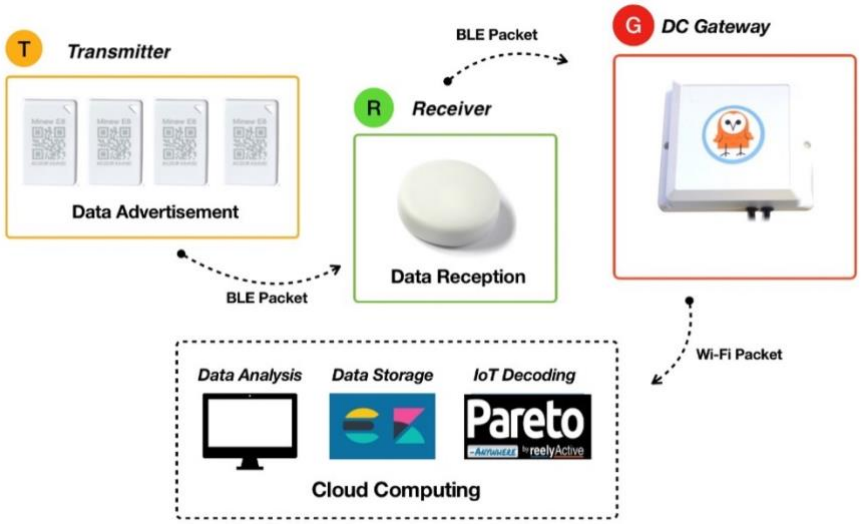

(a) Overview of Communication Architecture of the Proposed System.

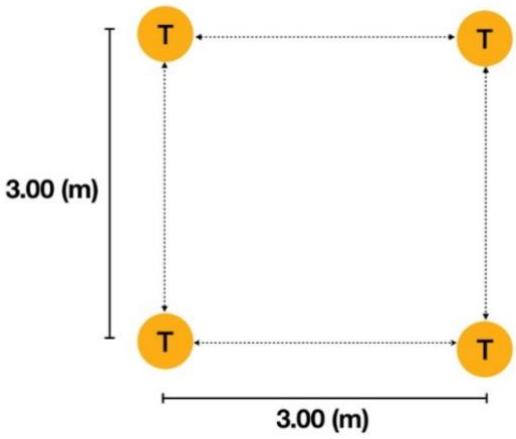

(b) The sub-module.

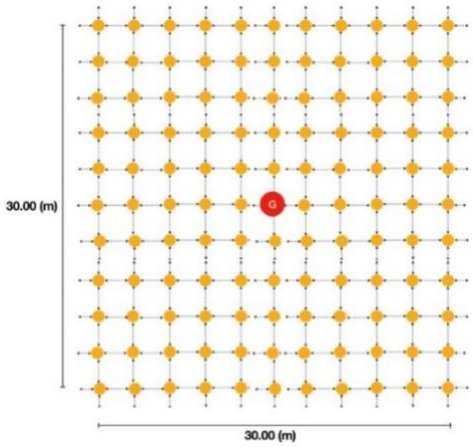

(c) A module composed of 100 submodules and one Gateway.

Figure 1: Overview of communication architecture of the proposed system and plan view of the hardware infrastructure.

3.2 Infrastructure Placement Strategies

This study proposes a modular placement system consisting of repetitive modules similar in size, shape, and device placement to distribute the RTLS infrastructure according to the site layout. The modules perform independently and are placed as required for site localization, however, they can be linked to each other to cover the entire construction site or zones of interest. Each module has a square shape composed of one gateway placed at its center, supporting a certain number of sub-modules. Each sub-module also has a square shape consisting of four fixed transmitters placed at its corners. The gateway sensing range constrains the module's size, and the sub-module dimensions are determined by the maximum distance in which the transmitting beacon can reach the receiving beacon and send BLE packets for the RSSI-distance prediction. We completed several experiments to

optimize the dimensions of submodules so that they maintain the expected level of accuracy, while minimizing the site installation requirements. Based on the results, some of which can be seen in (Khazen et al., 2022), the module with a side of 30 m and the sub-model with a size of 3.00 m are proposed. Figure 1 (b-c) illustrates the top view of the sub-module and the module. Increasing the density of BLE sub-modules, has been shown to enhance the system's accuracy by reducing signal interference and improving the robustness of proximity detection. This could be particularly valuable in complex construction environments and congested job sites with severe LoS blockages and/or magnetic fields and other forms of noise.

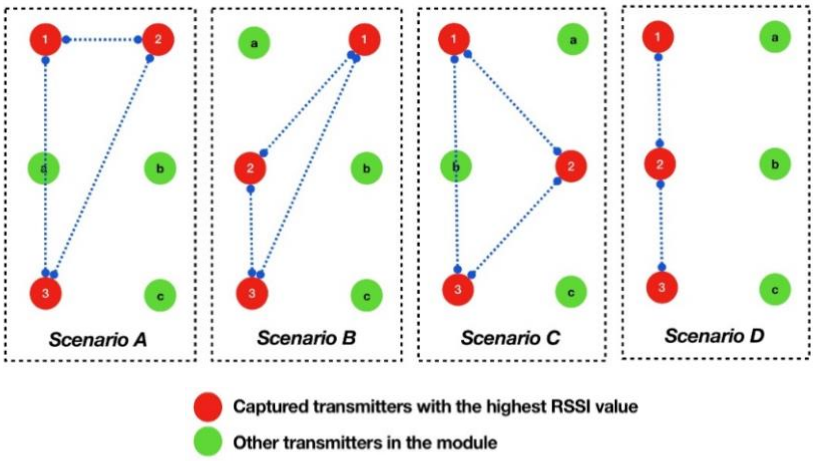

(a) Possible scenarios for the Semi-logical records.

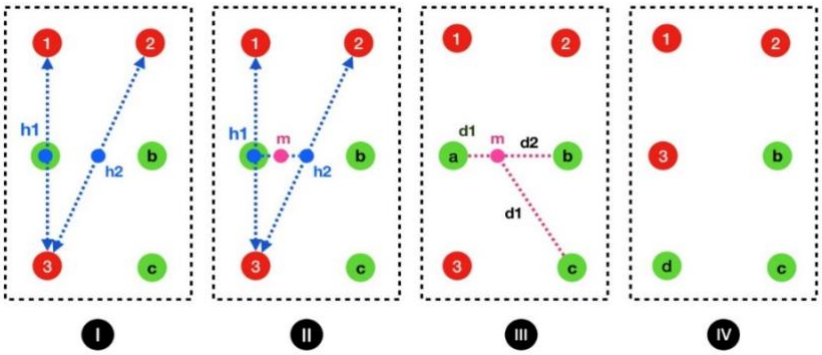

(b) The processes in the records correction algorithm: (i) Calculating middle points between the third transmitting beacon and the other two transmitters (ii) Determining the guide point (iii) calculating the distance between the guide point and the transmitter (iv) Predicted transmitting beacon replacement.

Figure 2: Possible scenarios for the Semi-logical records and the processes in the records correction algorithm.

The collected RSSI measurements with respect to the three transmitters are recorded with their respective timestamp that indicates the time it was created. On average, the RTLS generates a record every 1.7 seconds with a standard deviation of 0.7 seconds. Since the records sometimes contain transmitters that do not belong to a sub-module, they can be categorized based on the location of their reference transmitter in a module. This can help classify the records based on the concentration level of their transmitters' position in the module. The more concentrated the transmitters of a record are, the more trustable the records will be for the localization model to estimate the location of the target node. Thus, based on the level of concentration of the transmitters in records, they are categorized as (i) *Logical*, i.e., a record whose three broadcasted transmitters belong to the same sub-module, and the maximum allowable distances between the transmitters are equal to or less than the diagonal

length of the sub-module; (ii) *Semi-logical*, i.e., a record that fulfills the 'Logical' requirement for the pair of the two strongest transmitters, and the scenarios but not the third transmitting beacon; and finally, (iii) *Non-logical*, i.e., a record that belongs to neither Logical nor Semi-logical record. Figure 2 (a) depicts the four possible scenarios for Semi-logical records.

3.3 Software Solutions for Semi- or Non-logical Records

When a receiving beacon is located in a sub-module, the transmitters of that sub-module are expected to be the closest. In practice, however, sometimes receivers capture stronger signals from transmitters farther away than the closest ones, generating records with scattered transmitters not necessarily belonging to the same sub-module. This can happen due to the 'multipath', which strongly affects the propagation of BLE signals and contributes to RSSI fluctuations (Cantón Paterna *et al.*, 2017). The result will be Semi- or Non-logical records, which must be reduced as much as possible, to avoid confusion for localization algorithms. A novel algorithm is developed to convert Semi-logical records to Logical ones and accordingly mitigate the impacts of multipath. Figure 2 (b) shows the processes involved in the record correction algorithm. In order for a Semi-logical record to be converted to a Logical one, the third broadcasted transmitting beacon should be substituted with the one which belongs to the same module as the other two transmitters. The substitution of the third transmitting beacon is made by applying a set of processes on the Semi-logical records. Firstly, the algorithm calculates midpoints (X_{h1},Y_{h1}) and (X_{h2},Y_{h2}) of the lines connecting the third transmitting beacon (X_3,Y_3) to the other two (X_1,Y_1) and (X_2,Y_2) (see Figure 2 (b)). Then, the middle point between the previously found midpoints is calculated (X_m,Y_m). This point acts as a guide to specify the approximate area where the third transmitting beacon should reasonably be located. In the next step, distances between the guide point and transmitter in the neighborhood (except those already included in the record) are calculated. The transmitting beacon whose distance from the guide point is minimum is considered the correct third transmitting beacon in the record. In the final step, the correct transmitting beacon replaces the old one by keeping its RSSI value. The preserved RSSI value is associated with the old transmitting beacon, which is not necessarily the same as the RSSI of the replaced (correct) transmitting beacon. However, this can be used as the best approximation for the RSSI value of the replaced (correct) transmitting beacon. The algorithm's processes are shown in Appendix A.

3.4 RSSI-distance Prediction Model

For the Locating System to correctly identify the receiving beacon's location, the RSSI values captured from the three transmitters must be reliably translated into physical distances. To collect the dataset for training an RSSI-distance relationship, the receiving beacon was tested at 25 reference points (stations) marked in 25 cm intervals on a straight line with a 6.00 m total length. Since, in practice, the workers may keep (or wear) the receiving beacon beacons in various orientations or even carry them in their pockets, the experiments were performed for four orthogonal orientations of the transmitting beacon with respect to the receiving beacon. The number of RSSI records at each station, considering all the orientations, was around 300, and the total number of RSSI records for the experiment was 7,531.

Before training the model, outliers caused by the environmental noise were identified based on their distance from their nearest RSSI records and were eliminated from the dataset. Each record is ranked based on its distance to its 70th nearest neighbor, and the top records in this ranking are considered to be outliers. Based on trial and error, on the reference of a Random Forest (RF) model performance, the number of strongest outliers removed per distance and from the training set were found as 12 and 300 respectively. Fig. 3 (a) shows the removed outliers as orange dots. After that, the RSSI records were normalized through z-transformation since the machine learning ML model used in this study for training RSSI–distance relationship (i.e., RF) is distance-based (Iqbal *et al.*, 2018). The average and standard deviation (SD) of the values were calculated, and the scaled values were calculated by Z = (x – Avg.) / SD, so the average value and the standard deviation of the RSSI values were transformed to 0 and 1, respectively.

While different statistical and machine learning models, including Random Forest (RF), Gradient Boosting Decision Tree, Generalized Linear Regression (GLR), and k-Nearest Neighbours (kNN), were tested for training the attenuation equation (Details can be found in Khazen et al., 2022), RF model provided the best results in this study based on the results of a 5-fold cross-validation. The trained model achieved the Mean Absolute Error (MAE) and Root Mean Square Error (RMSE) of 0.507 (m) and 0.671 (m) in RSSI-distance prediction, respectively.

3.5 Localization Estimation Model

The localization estimation model can encounter various scenarios depending on the distances estimated between transmitters and the receiving beacon. Hence, the arrangement of circles representing the estimated distance of the receiving beacon from the transmitter and the coordinates of the transmitter should be determined first. The receiving beacon's location is calculated through a separate algorithm in the localization model for each possible arrangement. Given three estimated distances, i.e., r1, r2, and r3, between the transmitter t1 through t3, and the target node (receiving beacon), three circles, i.e., C1, C2, and C3, can be drawn. The center point of these circles is the known position of the reference transmitter. Their radii are equal to the estimated distances between the target node and the transmitter. To better clarify the localization model, the scenarios, along with their corresponding algorithm to estimate the target node's location are discussed separately in the following.

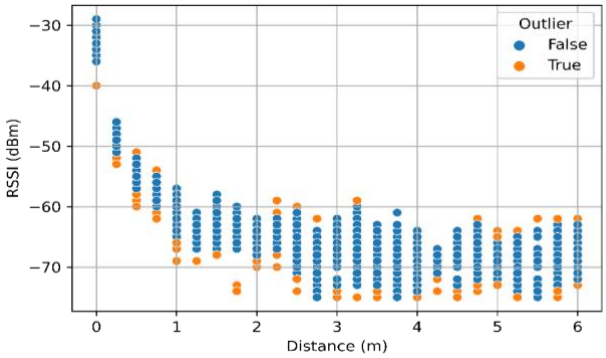

(a) Scatter plot showing the removed outliers.

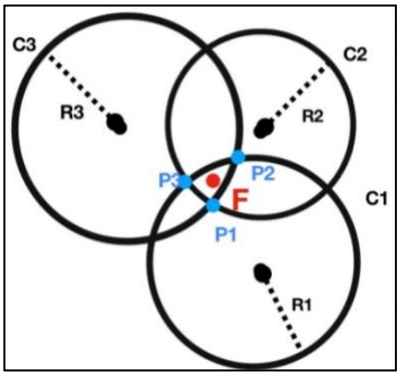

(i) Scenario (a).

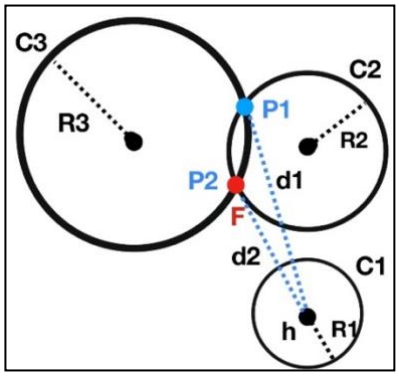

(ii) Scenario (b).

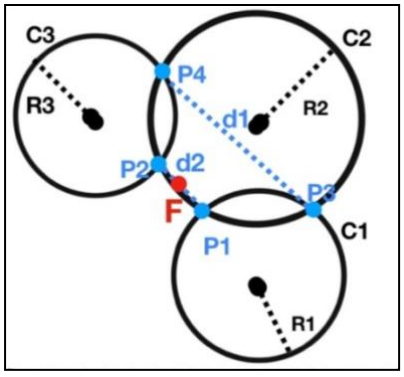

(iii) Scenario (c).

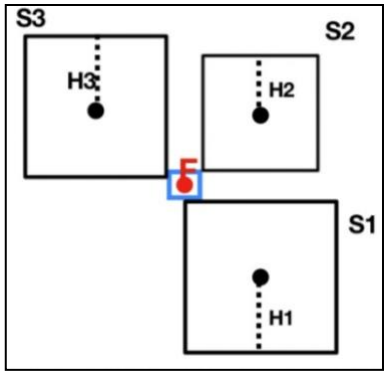

(iv) Scenario (d).

(v)

(b) Scenarios of different arrangements for triangulation.

Figure 3: Details of the RSSI-distance prediction model and the localization estimation model.

3.5.1 Scenario (a) three overlapping circles

There is an area of overlap among the three circles (Figure 3 (b) - Scenario a). In this scenario, the target location is estimated as the centroid of the intersection area, created by the three points P1, P2, and P3 using the following formula (1):

$$F_x = \frac{P1_x + P2_x + P3_x}{3}$$
$$F_y = \frac{P1_y + P2_y + P3_y}{3} \quad (1)$$

3.5.2 Scenario (b) two overlapping and one isolated circles

When only two circles overlap in an area, and the third circle is isolated (Figure 3 (b)- Scenario b); after determining the intersection points P1 and P2, the distances (d1 and d2) from the center of the isolated transmitting beacon, i.e., h, to the two intersection points are calculated. Then, the final estimated location of the target is the point whose distance (to the isolated circle's center) is shorter.

3.5.3 Scenario (c) two circles overlapping the third, but not one another

The scenario is that one circle (C2) intersects with the other two circles (C1, C3), but C1 and C2 themselves do not intersect (Figure 3 (b)- Scenario c). The intersection points P1 through P4 are calculated between the circles in this scenario. Then, the distances d1 and d2 between the intersection points of the separate circles (C1, C3) are calculated by equations (2) and (3). Finally, using equation (4), the midpoint F on the shorter distance (d1) is chosen as the final estimated location of the target beacon.

$$d1 = \sqrt{(P4_X - P3_X)^2 + (P4_Y - P3_Y)^2} \quad (2)$$

$$d2 = \sqrt{(P2_X - P1_X)^2 + (P2_Y - P1_Y)^2} \quad (3)$$

$$F_x = \frac{P1_x + P2_x}{2}$$
$$F_y = \frac{P1_y + P2_y}{2} \quad (4)$$

3.5.4 Scenario (d) Three isolated circles

In rare cases, there are three short coverage areas whose corresponding circles do not intersect. The arrangement of the circles in this scenario is demonstrated in Figure 3 (b)- Scenario d. For this scenario, the target beacon constructs a bounding box around each transmitting beacon, where the transmitting beacon is placed at the center, and the edge length of the bounding box is twice its estimated distance. The target beacon determines the intersection of the boxes, with boundary locations given by $x_{\min}$, $x_{\max}$, $y_{\min}$, and $y_{\max}$ which are calculated from equations (5) through (8). Finally, the center point of this intersection box is considered as the estimated target location (x_{est} and y_{est}) which are calculated by equations (9) and (10). Since the circles do not intersect in this scenario, this technique creates a hypothetical box whose edges are circumscribed by the edges of the transmitting beacons' bounding boxes.

$$x_{min} = max(x_1 - d_1, x_2 - d_2, x_3 - d_3) \quad (5)$$

$$x_{max} = min(x_1 + d_1, x_2 + d_2, x_3 + d_3) \quad (6)$$

$$y_{min} = max(y_1 - d_1, y_2 - d_2, y_3 - d_3) \quad (7)$$

$$y_{max} = min(y_1 + d_1, y_2 + d_2, y_3 + d_3) \quad (8)$$

$$x_{est} = \frac{(x_{min} + x_{max})}{2} \quad (9)$$

$$y_{est} = \frac{(y_{min} + y_{max})}{2} \quad (10)$$

To provide clarity on the proposed algorithm, the main steps of the localization estimation process are outlined in Appendix B.

3.6 Estimated Locations Post-Processing Model

Reflection and diffraction attributed to the presence of walls and floor (objects) within the indoor environment can produce multipath and fading effects, respectively. This can cause distortions in the estimated distances between the receiver and transmitter, resulting in noise for the location data of a target node (receiver) (Takenga *et al.*, 2007). Therefore, the estimated locations are post-processed to minimize the effect of distortions on the location of the target node. Two post-processing steps are performed in this study, which will be explained in the following.

3.6.1 Shifting the estimated location to the strongest transmitting beacon

The localization model considers the transmitting node whose signal is received with the highest RSSI value as the closest and most reliable transmitting beacon for localization. Accordingly, the estimated location of the target node will be shifted toward the location of that transmitting beacon. Firstly, the associated pair-wise weights between the estimated distances of the target node from the first and second transmitter received with the highest RSSI value are computed. It is noted that the RSSI-distance model occasionally predicts the distance between the receiving beacon and the transmitting beacon with the highest RSSI value longer than the one with the second-highest RSSI value. Given the two distances d_1 and d_2 as the estimated distances between the worker and the two transmitters, sorted ascendingly, the weights are calculated as follows:

$$w = \frac{d_2}{d_1} \tag{11}$$

Where d_1 is the estimated distance between the target node and the closest transmitting beacon and d_2 is the estimated distance between the target node and the second closest transmitting beacon. Then, the following equations are used to adjust and estimate the final location of the target node for all the scenarios.

$$x_{fin} = \frac{location\_X + X1 * w}{1 + w} \tag{12}$$

$$x_{fin} = \frac{location\_X + X1 * w}{1 + w} \tag{13}$$

Where $location\_X$ and $location\_Y$ are the coordinates of the estimated location by the localization model, and $X1$ and $Y1$ are the coordinates of the location of the strongest transmitting beacon.

3.6.2 Applying filtering

After shifting the estimated location to the strongest transmitting beacon, three filtering techniques are applied to smooth the locations' calculations. They include Simple Moving Average (SMA), Exponential Smoothing (ES), and Kalman Filtering (KF). These techniques are used as KF proved to have enough accuracy, and the other techniques (SMA and ES) provided low computation time. However, particle, particle Markov chain, Gaussian Sum Filtering, and other variants of Kalman have been deployed in previous studies (Malekzadeh *et al.*, 2020),(Sou *et al.*, 2019).

SMA is the most common filtering algorithm implemented in localization tasks. Despite its simplicity, it reduces random noise while retaining a sharp step response (Smith, 1999). A filtered record is calculated as the average of values within a symmetric window of size N around that record, where N is the pre-defined size of the window of the MA filtering (Mackey *et al.*, 2020). It is given as:

$$record_{MA} = \frac{\sum_{i=1}^{N} record_i}{N} \tag{14}$$

The second technique used in this study, ES, is one of the most popular and easy-to-use filtering methods (Ravinder, 2016). The basic formula of exponential smoothing is (Ji *et al.*, 2012):

$$S_t = \alpha x_t + (1 - \alpha) S_{t-1} \tag{15}$$

where S_t is the smoothed location at time t, x_t is the actual observation location at time t, S_{t-1} is the smooth location at time $t - 1$, and α is the smoothing constant with a domain between 0 and 1. The accuracy of the exponential smoothing model mainly depends on the selection of α.

The third tested technique was KF, which uses noisy observed data and data with other inconsistencies to estimate unknown states by the use of a mathematical model. KF was originally introduced by Kalman to solve the discrete-data linear filtering problem (Kalman, 1960) and has been used ever since by several studies for localization. KF filter is a standard optimal estimation algorithm based on Bayesian filter theory (Gupta *et al.*, 2021). It has two

stages, prediction and update (correction). Firstly, the filter predicts the next state at time t based on the current state at time (t-1) before the next state is made. The second stage computes a gain value G(t)based on the prior noise estimate. It then updates the posterior state and system noise estimations using the latest state observation and current gain value (Mackey *et al.*, 2020). In our study, the target node (the location of a worker) is described by four parameters (state variables), which can be written in a state vector as follows:

$$\boldsymbol{x} = [\mathrm{x}, \mathrm{x\_vel}, \mathrm{y}, \mathrm{y\_vel}] \tag{16}$$

where x and y are the cartesian coordinates of the target node and x_vel and x_vel are the velocities in the x and y directions. The (x,y) coordinates are set as the starting location of the target, and the velocity is set to 0 as the initial value for our experiment (Cantón Paterna *et al.*, 2017). The dynamics for each of our states in the current record "t" as a function of states in the previous record " t-1 " are given as the following equations:

$$\mathrm{x}(t) = \mathrm{x}(t-1) + \mathrm{dt} * \mathrm{x\_vel}(t-1) \tag{17}$$

$$\mathrm{x\_vel}(t) = \mathrm{x\_vel}(t-1) \tag{18}$$

$$\mathrm{y}(t) = \mathrm{y}(t-1) + \mathrm{dt} * \mathrm{y\_vel}(t-1) \tag{19}$$

$$\mathrm{y\_vel}(t) = \mathrm{y\_vel}(t-1) \tag{20}$$

where dt represents the change in time (time-step), and it is assumed that (x, y) coordinates are updated based on the current location and velocity. The formulas can be rewritten in matrix format as:

$$\mathbf{x}\,(t) = \mathbf{F} \times \mathbf{x}\,(t-1) \tag{21}$$

where:

$$\boldsymbol{F} = \begin{bmatrix} 1 & dt & 0 & 0 \\ 0 & 1 & 0 & 0 \\ 0 & 0 & 1 & dt \\ 0 & 0 & 0 & 1 \end{bmatrix} \tag{22}$$

Besides, the state covariance P indicates how much the state variables influence each other's values, determining the system's dependency on the initial state values. The values of the initial matrix **P**, i.e., (n), indicate the level of uncertainty that is considered for the estimated state (in this case, the location estimated by RTLS):

$$\boldsymbol{P} = \begin{bmatrix} n & 0 & 0 & 0 \\ 0 & n & 0 & 0 \\ 0 & 0 & n & 0 \\ 0 & 0 & 0 & n \end{bmatrix} \tag{23}$$

The measurement matrix **H** relates the measurements to the states' variables. **z** is the measurement vector, and **X** is the states' variables vector. The H function is used to obtain from the state variables vector x the values (in this case, the location) that are being measured (Cantón Paterna *et al.*, 2017):

$$\boldsymbol{z} = [x, y] \tag{24}$$

$$\boldsymbol{z} = \boldsymbol{H}x \tag{25}$$

$$\boldsymbol{H} = \begin{bmatrix} 1 & 0 & 0 & 0 \\ 0 & 0 & 1 & 0 \end{bmatrix} \tag{26}$$

This study examined two post-processing variants to smooth the estimated locations, namely 'mild' and 'intense'. Table 5 shows the parameter values used for the post-processing techniques at each level.

Table 6: The parameters changed for the post-processing levels.

Post-Processing Technique	Filtering Technique	Mild Post-Processing	Intense Post-Processing
Shifting the estimated location	–	w (weight) = 0.2 * W	w (weight) = 1 * w
Filtering technique	Exponential smoothing	α (alpha) = 0.3	α (alpha) = 0.8
	Simple moving average	neighbors = 20 records	neighbors = 6 records
	Kalman	observation covariance = (5 x previous estimated value)	observation covariance = (2000 x previous estimated value)

4. RESULTS AND DISCUSSION

The experimental study and analysis of the proposed RTLS focused on the potential factors that can affect the system's performance, including (i) the post-processing (smoothing) intensity level and (ii) Identifying the ideal position of the receiver on the workers. We tested three placements of the BLE beacons on workers, including (i) on the hardhat, (ii) on the chest, and (iii) on the wrist.

The system localization accuracy is examined against the effects of the post-processing techniques/intensity, filtering techniques, localization, and placement of the receiving beacon on different human body parts. The distance error between the ground truth location and the estimated location is computed using the Mean Absolute Error (MAE):

$$\text{Error } = \sqrt{(x_{\text{calc}} - x_{\text{real}})^2 + (y_{\text{calc}} - y_{\text{real}})^2} \tag{27}$$

where x_{calc} and y_{calc} are the coordinates of the target's estimated location, and x_{Real} and y_{Real} are the actual coordinates of the target.

Results were compared versus the benchmark case of placing the receiving beacon on a tripod at the same level as the transmitter. Details of the comparative study will be discussed elsewhere. However, the hardhat placement was used in this study for tracking workers due to the better Line-of-Sight for the receiver, hence showing closer results to the benchmark scenario, as will be explained later in this section.

4.1 Testbed Environment and System Setup

An in-lab experiment for analyzing the performance of the developed Locating System was conducted in a 9.00 m × 8.60 m area, referred to as the 'testbed', where computers, electronic devices, and magnetic fields were present. The lab environment provided an open space for testing and creating layouts to help simulate the effect of obstacles on the job site (see Figure 4 (a-b)). Two sub-modules, consisting of six transmitters, were deployed in the experiment. The receiving beacon, placed on top of a construction helmet, acted as the target node. The experimental methodology comprises two scenarios, where the target node is static and dynamic, to obtain a reliable system performance evaluation. For the static scenario, 66 reference grid points (stations) located 0.60 m apart from one another were marked in the testbed to ensure the target node's exact position while analyzing the system's positioning accuracy. The number of records that the receiver captured from the transmitters at each station was around 35, and in total, 2,344 records were collected and processed.

The impact of metal on signal degradation is admitted by the literature (Mohsin, et al. (2019) and Cantón Paterna, et al. (2017) among several others) and cannot be ignored. Various metal objects were available in our testbed, e.g., see the metallic files in FIG 4 (b), as well as the reinforcement available in the slab and columns, and hence, our results are despite the availability of such noise in the test environment. Nevertheless, studying the exact impact of reinforcement and other metals commonly available on a construction site requires closer investigations in the future, particularly for applications where a high-accuracy localization is crucial.

As per the dynamic scenario, the receiver captured signals while closed-loop trajectory paths were walked continuously at various speeds by the target node, as illustrated in Figure 4 (c-d). Two trajectory patterns were considered, and for each of them, the experiment was repeated three times with various speeds to obtain a reliable estimation of the system performance when the target node is dynamic. Since the number of turnings included in the trajectory pattern (I) is less than that of pattern (II), the target could travel pattern (I) at a higher speed. The records generated were 140 and 301 during the trajectory patterns (I) and (II), respectively. The actual records generated during the static and dynamic test scenarios are illustrated in Figure 4 (e-g).

We tested and evaluated the impact of various movement patterns on RTLS accuracy by tracking subjects performing different construction activities at varied speeds and body positions, including walking, stationary tasks, and transitions between work areas. Through the use of BLE beacons and accelerometers mounted on workers, the system captured fluctuations in signal strength due to body movements associated with primary tasks such as painting, plastering, and masonry, as well as secondary support activities. While movement patterns do introduce signal fluctuations, the RTLS system maintained relatively high accuracy in detecting location and identifying productivity states, albeit with some decline during more dynamic tasks. For further details on the setup and findings, readers are referred to (Khazen et al., 2024).

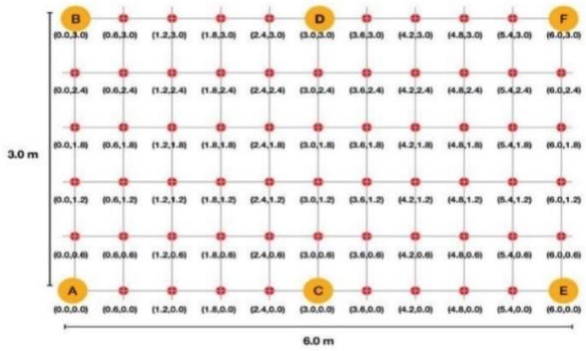

(a) *Placement plan of the devices and the reference points.*

(b) *View of the in-lab testbed.*

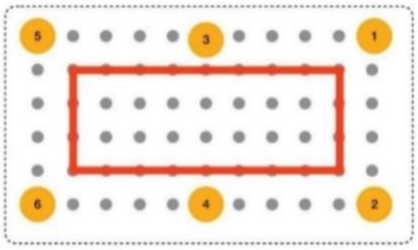

(c) *Trajectory pattern (i) considered for dynamic test scenario.*

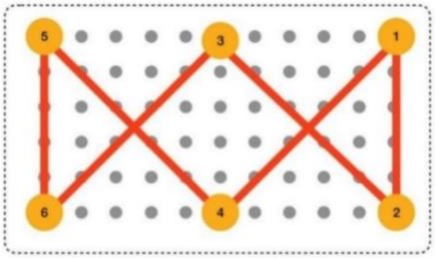

(d) *Trajectory pattern (ii) considered for dynamic test scenario.*

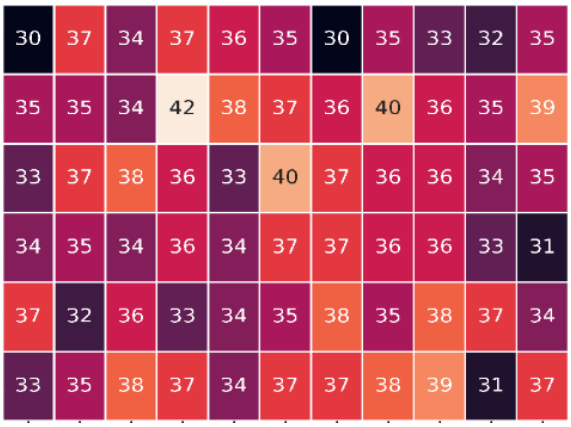

(e) *Heat map of the number of records received by the target node (receiver) at each station.*

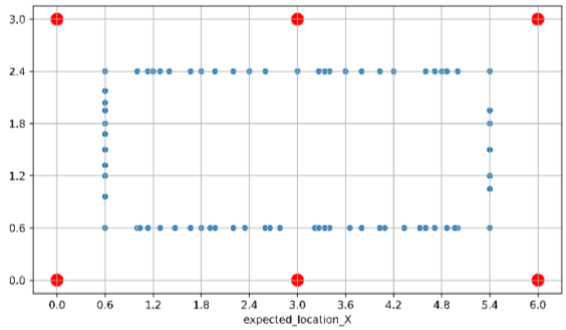

(f) *Actual locations of the records for the trajectory pattern (I).*

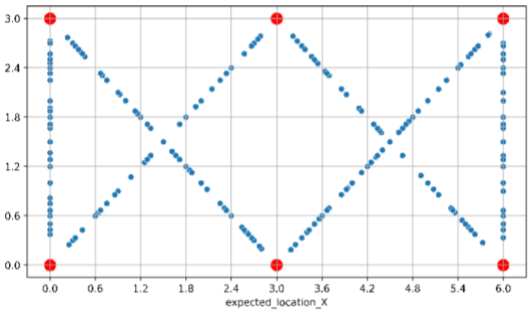

(g) *Actual locations of the records for the trajectory pattern (II).*

Figure 4: Details of the in-lab experiments (the axes of the heatmap and the scatter plots are in grid point (station) and meter, respectively).

4.2 Effects of the post-processing intensity on the system performance

This sub-section compares different intensity levels of post-processing on the localization accuracy for static and dynamic targets. In order to show the effectiveness of post-processing on the estimated locations, the system was also tested on the raw location data, i.e., without shifting the estimated locations and applying the filtering techniques. Table 7 shows the impacts of the different strength levels of post-processing on the localization accuracy for both experiment scenarios.

Table 8: Localization accuracy for the experiment scenarios with various post-processing methods.

Filtering Technique	***Applying "Intense" smoothing in post-processing***						***Applying "Mild" smoothing in post-processing***					
	Static		Dynamic				Static		Dynamic			
			Trajectory pattern (I)		Trajectory pattern (II)				Trajectory pattern (I)		Trajectory pattern (II)	
	MAE	*SD*	*MAE*	*SD*	*MAE*	*SD*	*MAE*	*SD*	*MAE*	*SD*	*MAE*	*SD*
Kalman	0.64	0.43	1.85	0.84	1.50	0.99	0.78	0.56	0.66	0.55	0.51	0.43
Moving Average	0.65	0.44	2.21	1.05	1.81	1.05	0.73	0.46	0.72	0.48	0.56	0.49
Exponential Smoothing	0.75	0.51	1.05	0.80	1.57	1.07	0.90	0.69	0.99	1.02	0.89	1.03
Raw Locations	1.04	0.82	1.18	1.12	1.03	0.93	1.04	0.82	1.18	1.12	1.03	0.93

As shown in Table 9, the least effective filtering technique could improve the accuracy of the raw estimated locations by around 28 percent by applying an "intense" smoothing, and the mean error can be reduced to as low as 0.64 m using the Kalman filter for the static test scenario. In sharp contrast, applying the Kalman filter's intense post-processing increased the mean error by 178 percent. Since the target does not move (for a short time) in a static scenario, the filtering techniques could leverage the previous records generated with a similar location, resulting in the minimized effect of noisy estimated locations by applying intense smoothing. However, the target movement in the dynamic test scenario had a significant negative impact on the effectiveness of applying intense filtering. It is evident from Table 10 that applying mild post-processing on the raw estimated locations for the dynamic test scenario could reduce the mean error from 1.18 m to 0.66 m and from 1.03 m to 0.51 m for the trajectory patterns (I) and (II), respectively. In the best scenario, the "Mild" strength level of post-processing achieved a mean error and SD of 0.51 m and 0.43 m, respectively, for the dynamic test scenario.

As per the static test scenario, a heatmap was produced to show the localization error of the static test experiment (under intense Kalman). The 66 grid points in the heatmap denote the test stations in the testbed. Regarding the dynamic test scenario, scatter plots of the distance error of the target's estimated locations in both trajectory patterns were created. Figure 5 (a) shows the heatmap of MAE of the estimated locations at each station, and Figure 5 (b-c) provides the scatter plots demonstrating the system's precision in the coverage area. As seen in Figure 5 (a), except for four test stations, the MAE of the rest of the stations is equal to or less than 1.00. The results shown in Figure 5 (b-c) conclude that the errors are uniformly distributed in the testbed except for the areas around the turn points. Hence, the system's accuracy does not have a bias toward a specific area of the testbed, including sub-module edges or areas close to the transmitters.

4.3 Discussion and Recommendations for Construction Sites

Based on the cost of deployment, the man-hours requirement for installing the RTLS infrastructure, the processing time, and the level of accuracy achieved, the authors conclude that deploying the proposed BLE-based RTLS is feasible for tracking workers on construction job sites. Deploying BLE beacons as the reference and tracking BLE devices help to minimize the interference to the workflow and safety implications resulting from cables of the wired sensors, and it also makes the RTLS infrastructure more resistant to fall damages. Since the location data are not collected nor transferred through the worker's smartphone, the data privacy issue is resolved in the developed RTLS. This issue is regarded as the most critical concern by workers in the adoption of tracking devices on job sites.

To further assess the resilience of the RTLS in the job site, future studies should involve experiments with reinforced concrete (RC) components such as columns, walls, and slabs in the testbed to simulate metal interference commonly encountered on construction sites. By positioning transmitters and receivers near the column, the setup could quantitatively evaluate the signal degradation and accuracy impact due to metal barriers.

Additionally, it would be valuable to investigate the effects of magnetic fields generated by metal components on BLE signal transmission and localization accuracy. Sensing and measuring these fields and using the readings as additional training data could provide insights into how magnetic interference influences the BLE tracking system, and beyond that can enable modification methods to the attenuation equation, based on the level of magnetic fields sensed on the site. While the accuracy of current RTLS fits general applications such as automated workspace monitoring and contact tracking among workers (for applicants as in pandemics); such improved tracking techniques can add a significant value for use cases that require a higher level of accuracy.

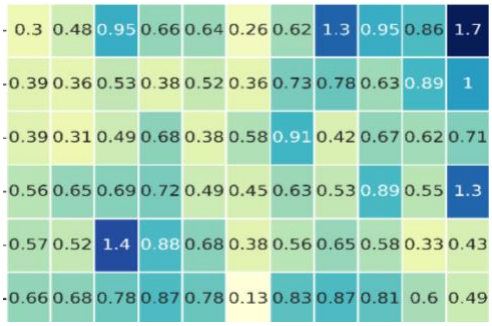

(a) Heatmap of MAE for the estimated locations at each station.

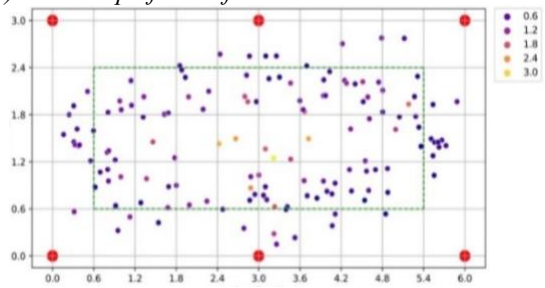

(b) Scatter plots of the system's precision in Trajectory pattern (i).

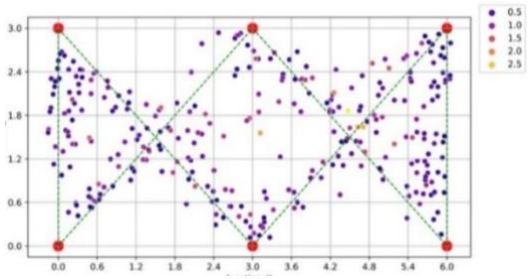

(c) Scatter plots of the system's precision in Trajectory pattern (ii).

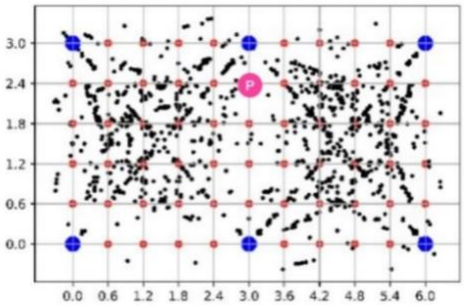

(d) Estimated locations – beacon on the tripod.

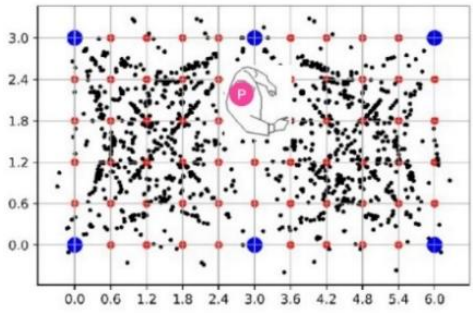

(e) Estimated locations – beacon was on the hardhat.

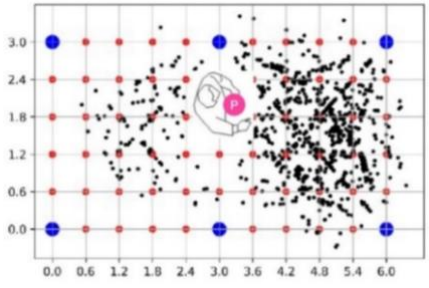

(f) Estimated locations – beacon was on the chest.

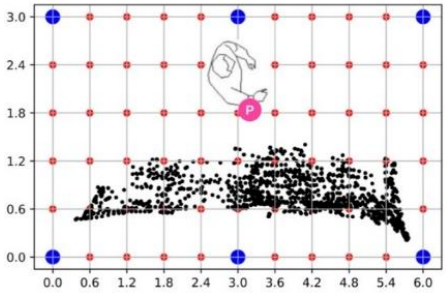

(g) Estimated locations – beacon was on the wrist.

Figure 5: Details of the experimental results.

Moreover, various intensity levels of the post-processing were found to be efficient for different applications, depending on the level of the worker's movement that each application requires monitoring. For instance, productivity assessment of crews involved in static operations, e.g., masonry work, carpentry welding, plastering, etc., requires an intense level of smoothing. Since the workers are not being relocated in short intervals, the filtering techniques can take advantage of their previous states' records to interpret their current state, which minimizes the error in the estimated locations. By contrast, mild smoothing is necessary for applications associated with workers' dynamic behavior, such as safety-related applications, including the deployment of safety alert systems for hazardous zone avoidance when approaching dangerous areas on the job site. A combination of mild and intense smoothing will be efficient for other applications in which the workers are both static and dynamic, such as automated workspace identification. As per the filtering type, Moving Average is the ideal alternative for safety-related applications due to its acceptable performance 95% of the time, and the shorter computation time than others, which will be essential for deploying real-time solutions. Although the Kalman filter roughly outperforms other filtering techniques in this study's evaluation metrics, it takes a significantly higher computation time, making it less appropriate for safety management applications than the Moving Average. However, the Kalman filter can be deployed successfully for productivity monitoring applications, including path planning and workspace identification.

For a successful RTLS deployment on the job sites, the following recommendations are made to enable a proper setup: (i) deploy the sub-module on the boundary of the area of interest (no need for a buffer area outside the target zone); (ii) distribute the sub-modules according to the site layout and keep on changing the position of the sub-module as the layout of the construction site changes during the project; (iii) consider the minimum size of the sub-module that is the maximum distance in which the transmitting beacon can send BLE packets reliably for RSSI-distance prediction throughout the localization. While the dimensions provided in this paper for the sub-modules reflect the maximum distances (given the hardware and software specifications of the system), in practice there are no limitations in lowering such dimensions, particularly when the site congestion or Non-Line-of-Sight (NLoS) issues challenge the RTLS accuracy; (iv) keep the transmitters at a minimum of height that is equal to the average of the worker's height, i.e. 2, or more in order for the beacons to have LoS with one another (increasing the height beyond that results in a shorter sub-module size); (v) turn the orientation of the transmitters towards the ground to provide an evenly transmission coverage area (particularly for job sites with many obstacles). Compared with recent studies, the developed RTLS outperforms them based on various performance metrics. The processing is relatively fast (nearly real-time); on average, the system generates a record every 1.7 seconds with a standard deviation of 0.7 seconds. The processing time for estimating a worker's location for 2,160 records is about 6.5 seconds. The low cost of devices is one of the essential advantages of the proposed system. As of 2022, the cost of system devices is estimated at $14 CAD for each transmitting beacon ($120 per 900 Sq.m); about $50 CAD for each receiving beacon (one per worker); and $150 CAD for each gateway (one per 900 Sq.m). Substitution of the commonly used reference devices (that cost as high as the gateways of the proposed RTLS) with affordable BLE transmitting beacon helped to reduce the RTLS implementation cost significantly. Compared with the literature (Li et al., 2019; Dinh, et al. 2020; Sun, et al., 2021a, among others), the proposed RTLS has been considered a superior solution in terms of costs on large construction sites that require a significant number of reference devices for RTLS.

The findings from this work offer implications for both researchers and practitioners. In terms of research contributions, this study validates that a system built entirely on beacons, eliminating the need for smartphones or complex gateway infrastructure, can effectively reduce both implementation costs and physical wiring requirements while enhancing on-site privacy protection. The developed record-correction algorithm, combined with adjustable smoothing parameters, establishes a methodological foundation that researchers can build upon to address various challenges, such as harsh environmental conditions, significant multipath interference, or applications demanding higher precision, including safety-critical operations. From an implementation perspective, this system provides construction management teams with an economical and minimally disruptive solution for workforce tracking that maintains data privacy without requiring workers to carry personal devices. The system's flexibility in smoothing intensity allows project teams to fine-tune their monitoring approach based on specific needs – whether that's real-time safety monitoring requiring rapid updates or longer-term productivity analysis benefiting from more stabilized data. The developed RTLS represents an advancement for the construction industry, offering a practical solution that successfully balances cost-effectiveness, measurement accuracy, and operational adaptability within the dynamic nature of construction environments.

5. CONCLUDING REMARKS

Tracking workers and objects on construction job sites is essential for various applications, including safety, progress monitoring, on-site coordination, and geographical mapping of worker locations and trajectories. The main goal of this study was to design a Real-Time Locating System for construction job sites by considering the aspects affecting the system deployability in the construction domain, including portability, affordability, scalability, and localization accuracy. Unlike traditional Bluetooth-based RTLS, in which smartphone or wired devices are included in the system architecture, this study uses wireless beacons as fixed and target nodes; hence there is no wiring except for the gateways. Furthermore, the modular infrastructure placement strategy proposed here proved the RTLS scalability and efficiency in terms of cost and power consumption. The strategy can be particularly beneficial in distributing the RTLS infrastructure according to the site layout to minimize the effects of NLOS between the transmitters and the receiver. The system also demonstrates no bias toward a specific coverage area and achieved, 90% of the time, an error of less than 1.17 for the test scenarios. Accordingly, the main contributions of this work can be summarized as (i) proposing an RTLS architecture with minimal dependency on wiring and electricity outlets; (ii) developing an algorithm and configuring receiving and transmitter to minimize the effect of signal interference caused by a network of transmitters; (iii) categorizing the measurements of positions and distances of the (fixed) transmitter from the (moving) receiver and developing localization algorithms for each category; and (iv) examining the performance of various post-processing mechanisms on the estimated locations to find the best solutions for mitigating the system's incoherence in computed locations when the target is static and dynamic.

Although this study highlights the feasibility of deploying BLE beacon technology as an RTLS, it has a few limitations that require further investigation. Firstly, since the experiments are conducted in a laboratory environment, the effect of distractions and noise, which generally exist in a construction environment, is minimized. Although the reference beacons are placed according to the layout of a building (e.g., walls, columns), the system might be vulnerable to the presence of movable obstacles (e.g., workers, equipment) in the RTLS coverage area due to the violation of LoS. Secondly, the body position of the worker wearing the receivers is assumed to be almost vertical in this experiment. The assumption can be valid for tracking workers in most activities; however, if the work involves physical movements of the worker's head, the accuracy of the RTLS could be affected due to the NLoS between the receiver and transmitters. Reducing the size of sub-modules of the tracking infrastructure can offer a potential solution in such cases. Thirdly, as per the filtering techniques, newer versions of Kalman filtering can be tested for location data post-processing in future research. Last but not least, the impact of various beacon configurations on the battery life is a practical factor for deployment that requires investigation.

ACKNOWLEDGMENT

This study was funded by the Natural Sciences and Engineering Research Council of Canada (NSERC), under ALLRP5539-85. The authors would also like to acknowledge the support of reelyActive company with respect to the equipment set up and validation of the results.

REFERENCES

Alishahi, N., Nik-Bakht, M., Ouf, M.M. (2021) A framework to identify key occupancy indicators for optimizing building operation using WiFi connection count data. Building and Environment. 200(May), 107936.

Becerik-Gerber, B., Siddiqui, M.K., Brilakis, I., El-Anwar, O., El-Gohary, N., Mahfouz, T., Jog, G.M., Li, S., Kandil, A.A. (2014) Civil Engineering Grand Challenges: Opportunities for Data Sensing, Information Analysis, and Knowledge Discovery. Journal of Computing in Civil Engineering. 28(4), 04014013.

Baek S.H. and Cha S.H. (2019). The trilateration-based BLE Beacon system for analyzing user-identified space usage of new ways of working offices, Building and Environment, Vol. 149, 264–274. DOI: https://doi.org/10.1016/j.buildenv.2018.12.030.

Bai L., Ciravegna F., Bond R. and Mulvenna M. (2020). A low-cost indoor positioning system using Bluetooth low energy, IEEE Access, Vol. 8, 136858–136871. DOI: https://doi.org/10.1109/ACCESS.2020.3012342.

Bencak P., Hercog D. and Lerher T. (2022). Indoor positioning system based on Bluetooth low energy technology and a nature-inspired optimization algorithm, Electronics, Vol. 11, Article 308. DOI: https://doi.org/10.3390/electronics11030308.

Cantón Paterna V., Calveras Augé A., Paradells Aspas J. and Pérez Bullones M.A. (2017). A Bluetooth Low Energy Indoor Positioning System with Channel Diversity, Weighted Trilateration and Kalman Filtering, Sensors, Vol. 17, Article 2927. DOI: https://doi.org/10.3390/s17122927.

Castillo-Cara M., Lovón-Melgarejo J., Bravo-Rocca G., Orozco-Barbosa L., and García-Varea I. (2017). An analysis of multiple criteria and setups for Bluetooth smartphone-based indoor localization mechanism, Journal of Sensors, Vol. 2017, Article ID 1928578, 22 pages. DOI: https://doi.org/10.1155/2017/1928578.

Cantón Paterna, V., Calveras Augé, A., Paradells Aspas, J., Pérez Bullones, M.A. (2017) A Bluetooth Low Energy Indoor Positioning System with Channel Diversity, Weighted Trilateration and Kalman Filtering. Sensors (Basel, Switzerland). 17(12).

Costin, A., Pradhananga, N., Teizer, J. (2012) Leveraging passive RFID technology for construction resource field mobility and status monitoring in a high-rise renovation project. Automation in Construction. 24, 1–15.

Dinh T.-M.T., Duong N.-S. and Sandrasegaran K. (2020). Smartphone-based indoor positioning using BLE iBeacon and reliable lightweight fingerprint map, IEEE Sensors Journal, In press, Article 2989411. DOI: https://doi.org/10.1109/JSEN.2020.2989411.

Dror E., Zhao J., Sacks R. and Seppänen O. (2019). Indoor tracking of construction workers using BLE: mobile beacons and fixed gateways vs. fixed beacons and mobile gateways, Proceedings of the 27th annual conference of the international group for lean construction (Pasquire C. and Hamzeh F.R., editors), Dublin, Ireland, 831–842. DOI: https://doi.org/10.24928/2019/0154.

Gómez-de-Gabriel J.M., Fernández-Madrigal J.A., López-Arquillos A. and Rubio-Romero J.C. (2018). Monitoring harness use in construction with BLE beacons, Measurement, Vol. 117, 144–152. DOI: https://doi.org/10.1016/j.measurement.2018.07.093.

Gupta, S., Singh, A.P., Deb, D., Ozana, S. (2021) Kalman filter and variants for estimation in 2dof serial flexible link and joint using fractional order pid controller. Applied Sciences (Switzerland). 11(15).

Huang K., He K., and Du X. (2019). A hybrid method to improve the BLE-based indoor positioning in a dense Bluetooth environment, Sensors, Vol. 19, No. 2, Article 424. DOI: https://doi.org/10.3390/s19020424.

Iqbal, Z., Luo, D., Henry, P., Kazemifar, S., Rozario, T., Yan, Y., Westover, K., Lu, W., Nguyen, D., Long, T., Wang, J., Choy, H., Jiang, S. (2018) Accurate real time localization tracking in a clinical environment using Bluetooth Low Energy and deep learning. PLoS ONE. 13(10), 1–13.

Ji, P., Xiong, D., Wang, P., Chen, J. (2012) A study on exponential smoothing model for load forecasting. Asia-Pacific Power and Energy Engineering Conference, APPEEC. (2).

Kalman, R.E. (1960) A new approach to linear filtering and prediction problems. Journal of Fluids Engineering, Transactions of the ASME. 82(1), 35–45.

Khazen, M., Nik-Bakht, M., & Moselhi, O. (2024). Monitoring workers on indoor construction sites using data fusion of real-time worker's location, body orientation, and productivity state. Automation in Construction, 160, 105327. https://doi.org/10.1016/J.AUTCON.2024.105327Khazen, M., Nik-Bakht, M., Moselhi, O. (2022)

Park J. and Cho Y.K. (2017). Development and evaluation of a probabilistic local search algorithm for complex dynamic indoor construction sites, Journal of Computing in Civil Engineering, Vol. 31, No. 4, 04017015. DOI: https://doi.org/10.1061/(ASCE)CP.1943-5487.0000658.

Proximity Detection on Construction Sites, Using Bluetooth Low Energy Beacons. Lecture Notes in Civil Engineering. 240, 215–226.

Li M., Zhao L., Tan D. and Tong X. (2019). BLE fingerprint indoor localization algorithm based on eight-neighborhood template matching, Sensors, Vol. 19, No. 22, Article 4859.

Kim, D., Liu, M., Lee, S.H., Kamat, V.R. (2019) Remote proximity monitoring between mobile construction resources using camera-mounted UAVs. Automation in Construction. 99(November 2018), 168–182.

Kim H. and Han S. (2018). Accuracy improvement of real-time location tracking for construction workers, Sustainability, Vol. 10, No. 5, Article 1488, pp. 1–16. DOI: https://doi.org/10.3390/su10051488.

Kunhoth, J., Karkar, A., Al-Maadeed, S., Al-Attiyah, A. (2019) Comparative analysis of computer-vision and BLE technology based indoor navigation systems for people with visual impairments. International Journal of Health Geographics. 18(1).

Kunhoth, J., Karkar, A.G., Al-Maadeed, S., Al-Ali, A. (2020) Indoor positioning and wayfinding systems: a survey. Human-centric Computing and Information Sciences. 10(1).

Mackey, A., Spachos, P., Song, L., Plataniotis, K.N. (2020) Improving BLE Beacon Proximity Estimation Accuracy Through Bayesian Filtering. IEEE Internet of Things Journal. 7(4), 3160–3169.

Malekzadeh, P., Mehryar, S., Spachos, P., Plataniotis, K.N., Mohammadi, A. (2020) Non-gaussian ble-based indoor localization via gaussian sum filtering coupled with Wasserstein distance. ICASSP, IEEE International Conference on Acoustics, Speech and Signal Processing - Proceedings. 2020-May, 9046–9050.

Mohsin, N., Payandeh, S., Ho, D., Gelinas, J.P. (2019) Study of Activity Tracking through Bluetooth Low Energy-Based Network. Journal of Sensors. 2019.

Montaser A. and Moselhi O. (2013). RFID indoor location identification for construction projects, Automation in Construction, Vol. 33, 128–137. DOI: https://doi.org/10.1016/j.autcon.2013.06.012.

Moselhi, O., Bardareh, H., Zhu, Z. (2020) Automated data acquisition in construction with remote sensing technologies. Applied Sciences (Switzerland). 10(8), 1–31.

Park, J., Kim, K., Cho, Y.K. (2017) Framework of Automated Construction-Safety Monitoring Using Cloud-Enabled BIM and BLE Mobile Tracking Sensors. Journal of Construction Engineering and Management. 143(2), 1–12.

Park, M., Asce, A.M., Koch, C., Brilakis, I., Asce, M. (2012) Three-Dimensional Tracking of Construction Resources Using an On-Site Camera System. . 26(August), 541–549.

Park, M.W., Brilakis, I. (2016) Continuous localization of construction workers via integration of detection and tracking. Automation in Construction. 72, 129–142.

Ravinder, H. v. (2016) Determining The Optimal Values Of Exponential Smoothing Constants – Does Solver Really Work? American Journal of Business Education (AJBE). 9(1), 1–14.

Sadowski S. and Spachos P. (2018). RSSI-based indoor localization with the Internet of Things, IEEE Access, Vol. 6, 30149–30161. DOI: https://doi.org/10.1109/ACCESS.2018.2843325.

Sattineni, A., Schmidt, T. (2015) Implementation of Mobile Devices on Jobsites in the Construction Industry. Procedia Engineering. 123, 488–495.

Smith, S.W. (1999) Digital Signal Processing, Chapter 15. California Technical Publishing, 277–284.

Sun X., Ai H., Tao J., Hu T. and Cheng Y. (2021). BERT-ADLOC: a secure crowdsourced indoor localization system based on BLE fingerprints, Applied Soft Computing, Vol. 104, Article 107237. DOI: https://doi.org/10.1016/j.asoc.2021.107237.

Sun D., Wei E., Ma Z., Wu C. and Xu S. (2021). Optimized CNNs for indoor localization through BLE sensors using improved PSO, Sensors, Vol. 21, No. 6, Article 1995. DOI: https://doi.org/10.3390/s21061995.

Sou, S.I., Lin, W.H., Lan, K.C., Lin, C.S. (2019) Indoor location learning over the wireless fingerprinting system with particle markov chain model. IEEE Access. 7(January), 8713–8725.

Taşkan A.K. and Alemdar H. (2021). Obstruction-aware signal-loss-tolerant indoor positioning using Bluetooth low energy, Sensors, Vol. 21, No. 3, Article 971. DOI: https://doi.org/10.3390/s21030971.

Takenga, C., Peng, T., Kyamakya, K. (2007) Post-processing of fingerprint localization using Kalman filter and map-matching techniques. International Conference on Advanced Communication Technology, ICACT. 3, 2029–2034.

Umer W. and Siddiqui M.K. (2020). Use of ultra wide band real-time location system on construction jobsites: feasibility study and deployment alternatives, International Journal of Environmental Research and Public Health, Vol. 17, Article 2219. DOI: https://doi.org/10.3390/ijerph17072219.

Zhao, J., Seppänen, O., Peltokorpi, A., Badihi, B., Olivieri, H. (2019) Real-time resource tracking for analyzing value-adding time in construction. Automation in Construction. 104(January), 52–65.

Zhuang, S. (2020) Real-Time Indoor Location Tracking in Construction Site Using BLE Beacon Trilateration.

Zhuang, Y., Yang, J., Li, Y., Qi, L., El-Sheimy, N. (2016) Smartphone-based indoor localization with bluetooth low energy beacons. Sensors (Switzerland). 16(5), 1–20.

APPENDIX A: SEMI-LOGICAL TO LOGICAL RECORD CONVERSION ALGORITHM

Input	:	Records = {user_id, $\text{Distance}_1, \text{X}_1, \text{Y}_1, \text{Distance}_2, \text{X}_2, \text{Y}_2, \text{Distance}_3, \text{X}_3, \text{Y}_3$, timestamp }//the collected records
Output	:	Records = {user_id, $\text{Distance}_1, \text{X}_1, \text{Y}_1, \text{Distance}_2, \text{X}_2, \text{Y}_2, \text{Distance}_3, \text{X}_3, \text{Y}_3$, timestamp }
Process 1	:	Define: //initial the mid-points of the lines connecting the strongest and second strongest transmitting beacons to the third transmitting beacon h_1 (x)= $\frac{(\text{X}_1+\text{X}_3)}{2}$, h_1 (y)= $\frac{(Y_1+Y_3)}{2}$ h_2 (x)= $\frac{(\text{X}_2+\text{X}_3)}{2}$, h_2 (y)= $\frac{(Y_2+Y_3)}{2}$
process 2	:	Calculate: //initial the mid-point between the points of h1 and h2 $m_x = \frac{(X_{h1}+X_{h2})}{2}$, $m_y = \frac{(Y_{h1}+Y_{h2})}{2}$
Process 3	:	Define: // initial the eligible transmitting beacons Tr_i ! = (Tr_1 & Tr_2 & Tr_3), (I ∈ R) Calculate: // calculate the distance between m and all the transmitting beacons $d_i = \sqrt{\left(m_x - Tr_{i(x)}\right)^2 + \left(m_y - Tr_{i(y)}\right)^2}$ Judge: //determine the transmitting beacon whose distance is shorter If $d_i > d_1 > d_2 > \ldots > d_n$, (n ∈ N) Select Tr_i
Process 4	:	Replace: // substitute the third transmitting beacon with the newly selected transmitting beacon (Tr_i <=> Tr_3)

APPENDIX B: PSEUDO-CODE FOR LOCALIZATION ESTIMATION MODEL

```
Input   : r1, r2, r3 : Estimated distances from transmitters t1, t2, t3
          (t1_x, t1_y), (t2_x, t2_y), (t3_x, t3_y) : Coordinates of transmitters
Output  : (x_est, y_est) : Estimated coordinates of the receiving beacon
Process : Begin
           // Scenario (a): Three Overlapping Circles
           If Circles C1, C2, and C3 Overlap Then
              Calculate Intersection Points (P1, P2, P3)
              x_est = (P1_x + P2_x + P3_x) / 3
              y_est = (P1_y + P2_y + P3_y) / 3
           EndIf

           // Scenario (b): Two Overlapping and One Isolated Circle
           If Only Two Circles Overlap Then
              Calculate Intersection Points (P1, P2)
              d1 = Distance from isolated circle center to P1
              d2 = Distance from isolated circle center to P2
              If d1 < d2 Then
                 (x_est, y_est) = P1
              Else
                 (x_est, y_est) = P2
              EndIf
           EndIf

           // Scenario (c): Two Circles Overlapping the Third, but Not Each Other
           If Two Circles Overlap a Third, But Not Each Other Then
              Calculate Intersection Points (P1, P2, P3, P4)
              d1 = Distance(P3, P4)
              d2 = Distance(P1, P2)
              If d1 < d2 Then
                 x_est = (P3_x + P4_x) / 2
                 y_est = (P3_y + P4_y) / 2
              Else
                 x_est = (P1_x + P2_x) / 2
                 y_est = (P1_y + P2_y) / 2
              EndIf
           EndIf

           // Scenario (d): Three Isolated Circles
           If No Circles Overlap Then
              x_min = max(t1_x - r1, t2_x - r2, t3_x - r3)
              x_max = min(t1_x + r1, t2_x + r2, t3_x + r3)
              y_min = max(t1_y - r1, t2_y - r2, t3_y - r3)
              y_max = min(t1_y + r1, t2_y + r2, t3_y + r3)

              x_est = (x_min + x_max) / 2
              y_est = (y_min + y_max) / 2
           EndIf

           Return (x_est, y_est)
          End
```